iScience, Volume *26*

Supplemental information

A modular hydrogel bioink containing microsphere-embedded chondrocytes for 3D-printed multiscale composite scaffolds for cartilage repair

Panjing Yin, Weiwei Su, Ting Li, Ling Wang, Jianying Pan, Xiaoqi Wu, Yan Shao, Huabin Chen, Lin Lin, Yang Yang, Xiulin Cheng, Yanbing Li, Yaobin Wu, Chun Zeng, and Wenhua Huang

Supplemental Information

A modular hydrogel bioink containing microsphere-embedded chondrocytes for 3D-printed multiscale composite scaffolds for cartilage repair

Panjing Yin, Weiwei Su, Ting Li, Ling Wang, Jianying Pan, Xiaoqi Wu, Yan Shao, Huabin Chen, Lin Lin, Yang Yang, Xiulin Cheng, Yanbing Li, Yaobin Wu, Chun Zeng, and Wenhua Huang

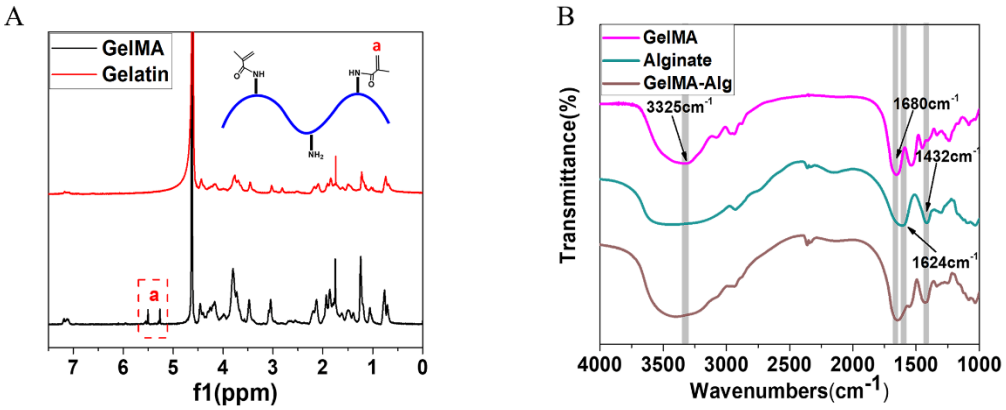

Figure S1. Characterization of materials, related to Figure 2. A.) ^{1}H NMR spectra of gelatin and gelatin methacrylate (GelMA). The peaks at 5.4 ppm and 5.6 ppm are assigned to the two protons in the methacrylate double bond. B.) Fourier transform infrared spectra of GelMA, alginate, and GelMA-alginate composite (GelMA-alg).

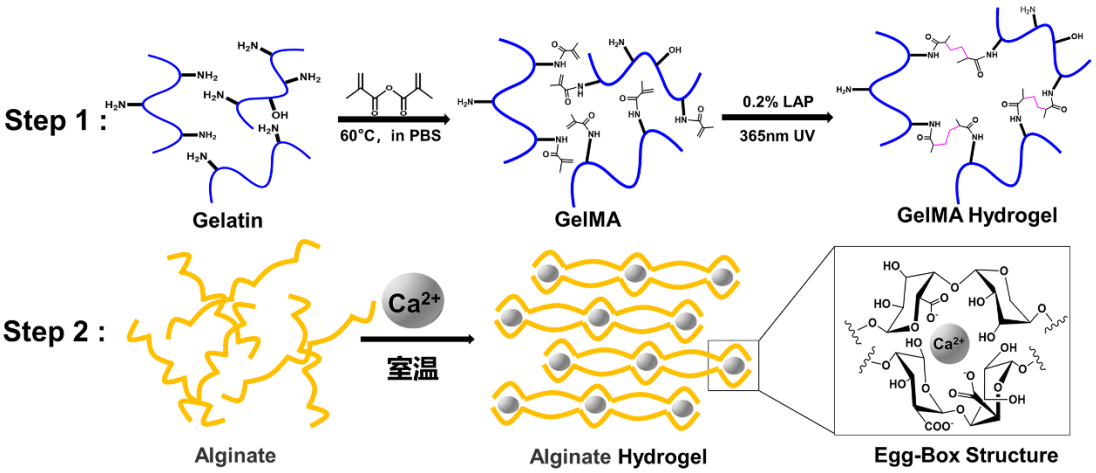

Figure S2. Synthetic scheme of the double cross-linking network formation of the GA hydrogel, related to Figure 2. Gelatin was reacted with methacrylic anhydride (MA) to form GelMA, which was subsequently cross-linked via UV irradiation to form a hydrogel (step 1), and alginate was cross-linked into a hydrogel by immersing in an aqueous solution with Ca^{2+} (step 2).

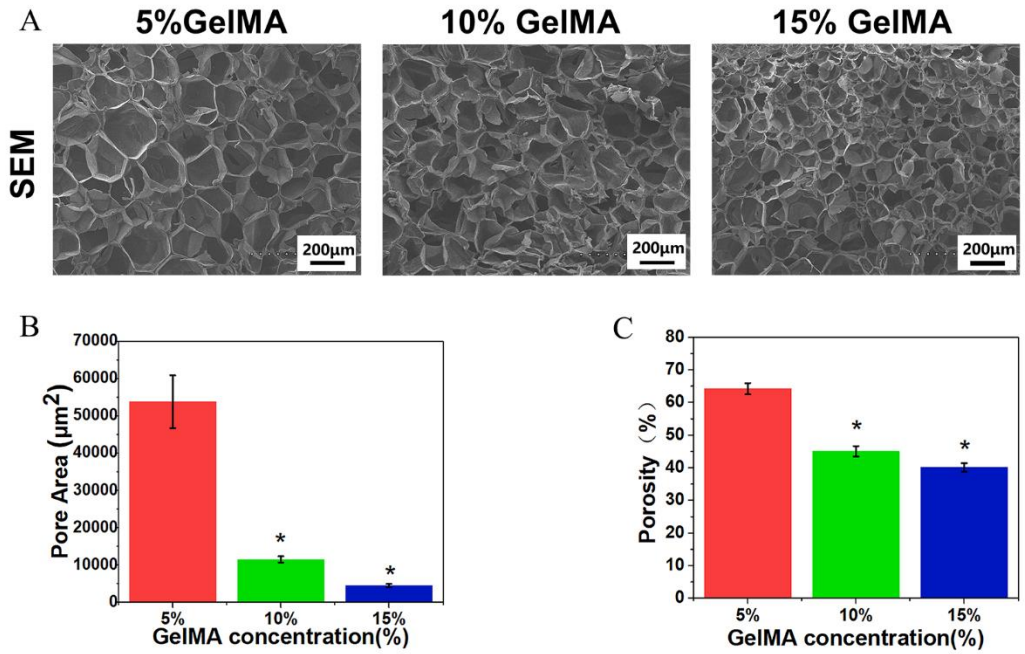

Figure S3. Characterization of GelMA at different concentrations (n = 3, n represents number of GelMA hydrogel samples), related to Figure 2. A.) Scanning electron microscopy images showing the inner structures of the GelMA hydrogels at different GelMA contents (5%, 10%, and 15% w/v). B.) Pore area and C.) porosity of the GelMA hydrogels. Statistical significance: *$p < 0.05$.

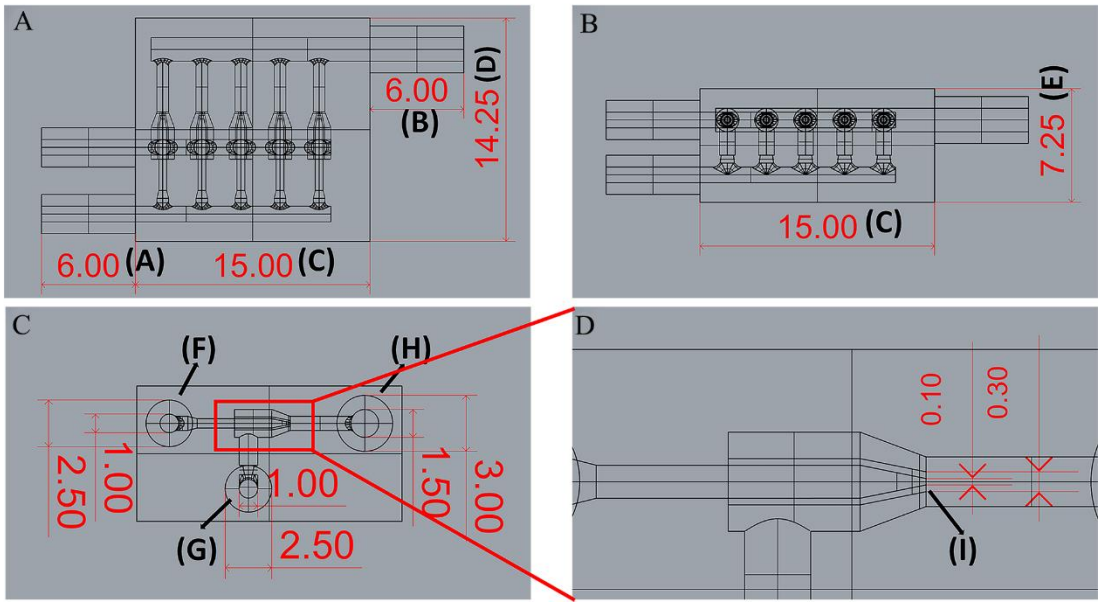

Figure S4. Design drawing of the multichannel microfluidic chip, related to Figure 3. A.) Top and B.) front, and C.) side views of the microfluidic chip design. D.) Schematic illustration of the inner and outer diameters of the inner phase channel in the microfluidic chip.

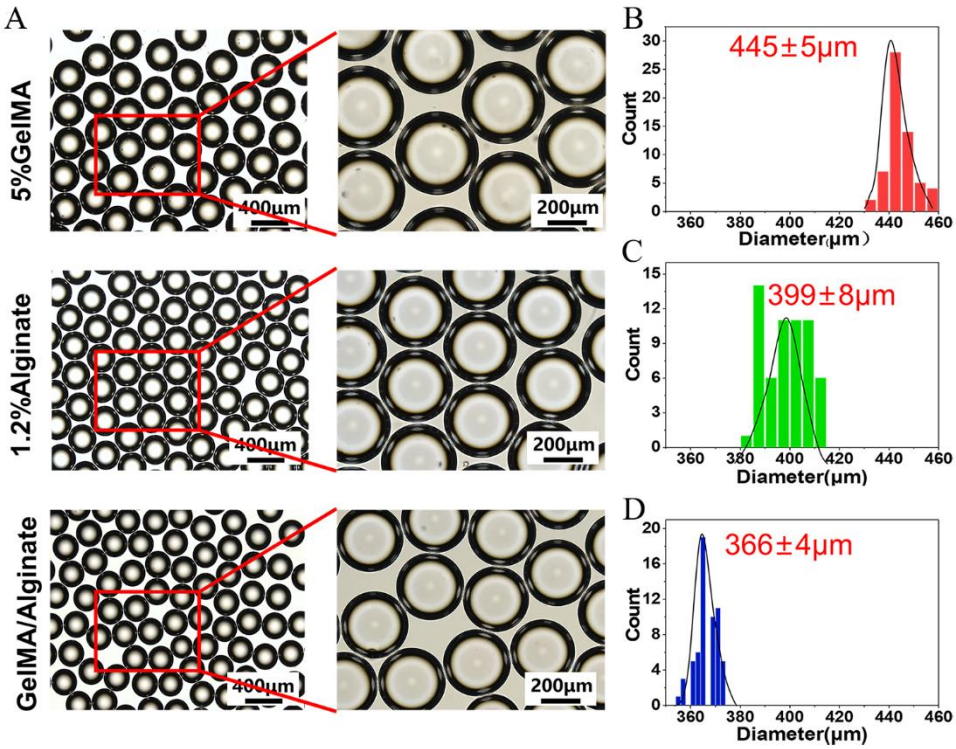

Figure S5. Microspheres were prepared using the microfluidic chip with different aqueous phases (n = 3, n represents number of GA-MS sample groups), related to Figure 3. A.) Diameters of microspheres prepared from GelMA, alginate, and GA samples. B-D.) Statistical distribution of microsphere diameters.

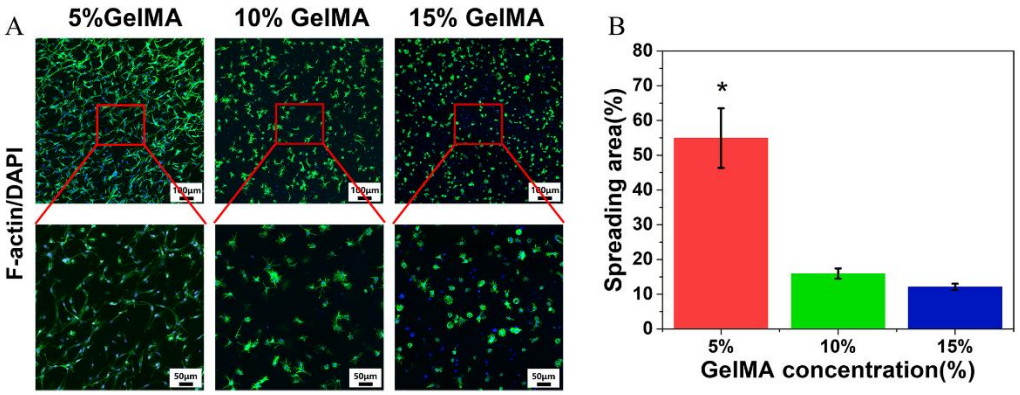

Figure S6. Chondrocytes were cultured within GelMA hydrogels at different concentrations (n = 3, n represents number of GelMA hydrogel samples), related to Figure 5. A.) Confocal images of F-actin/4′,6-diamidino-2-phenylindole (DAPI) markers from chondrocytes encapsulated in GelMA hydrogels with different GelMA contents (5, 10, and 15% w/v). B.) Spreading area of chondrocytes encapsulated in the GelMA hydrogels. Statistical significance: *$p < 0.05$.

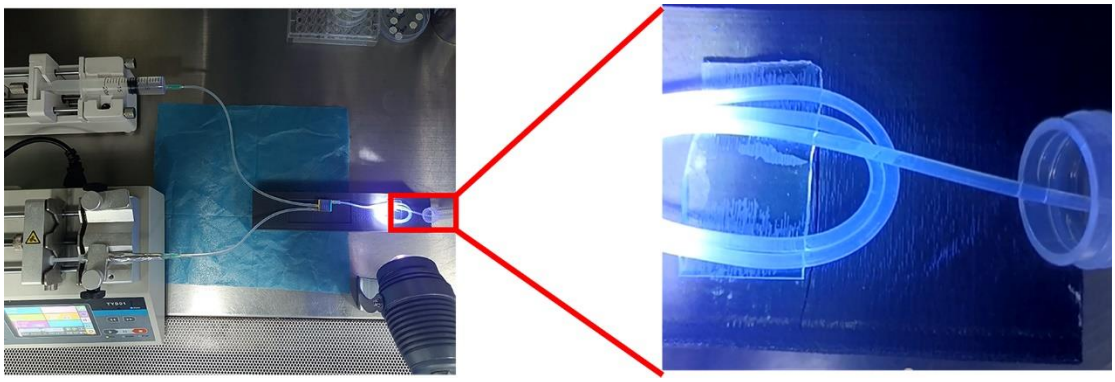

Figure S7. Preparation process of chondrocyte-encapsulated GA microspheres, related to Figure 5.

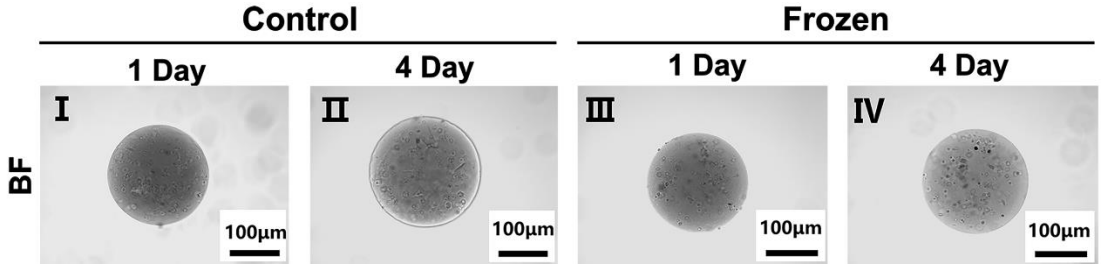

Figure S8. Optical micrographs of the chondrocyte-encapsulated GA microspheres from the control group (I and III) and frozen group (III and IV) after 1 and 4 d of culture, related to Figure 5.

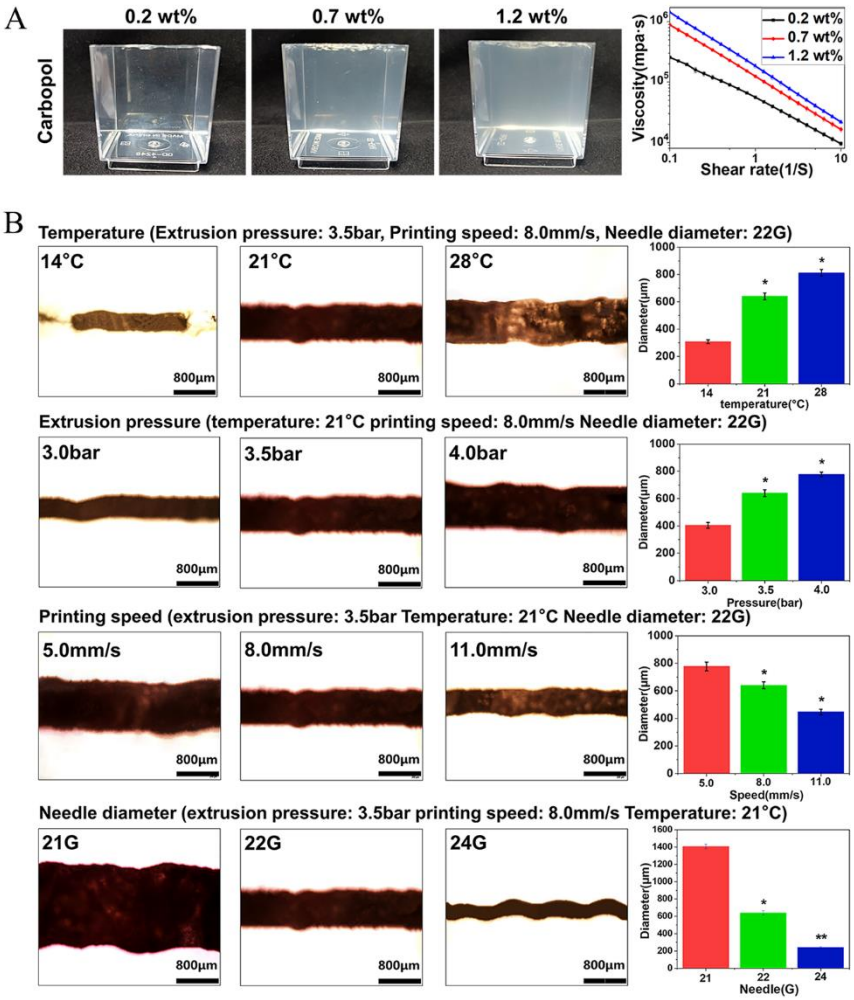

Figure S9. Dimensional stability of the hydrogel printed in a Carbopol support bath (n = 3, n represents number of scaffolds), related to Figure 6. A.) Photographs of the Carbopol support bath at different concentrations (0.2%, 0.7%, and 1.2% w/v) after bubble removal and their viscosities (shear rate ranged from 0.1 to 10 s^{-1}). B.) Images of wires printed by varying the temperature, extrusion pressure, printing speed, and needle diameter and statistics of the wire diameters. Statistical significance: *$p < 0.05$, **$p < 0.01$.

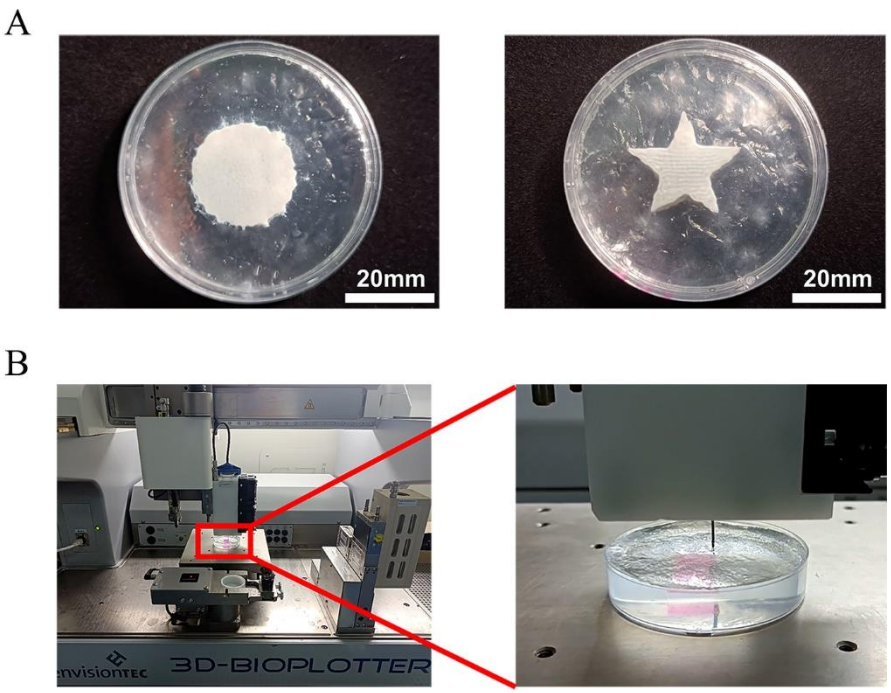

Figure S10. Precision of scaffolds prepared a Carbopol support bath, related to Figure 6. A.) Circular and star-shaped specimens printed in the Carbopol support bath under specific conditions (temperature: 21 °C, extrusion pressure: 3.5 bar, printing speed: 8.0 mm/s, needle diameter: 22G). B.) Photographs illustrating the printing of multiscale composite scaffolds in the Carbopol support bath using a 3D bioprinter.

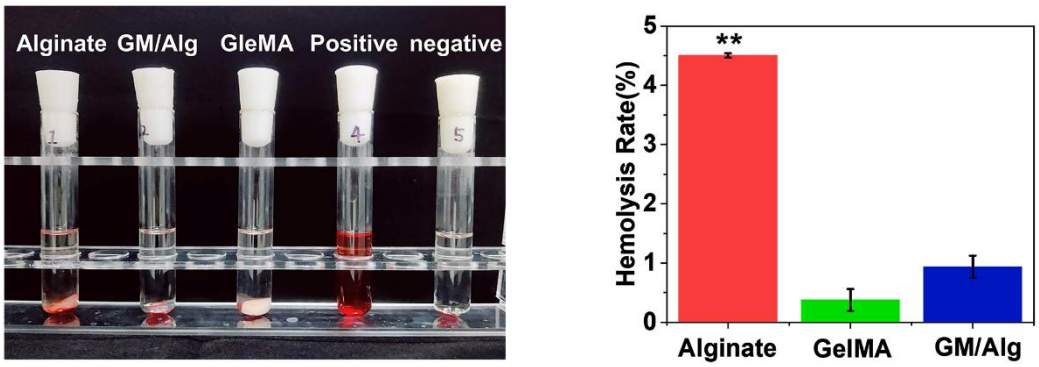

Figure S11. Hemolysis assay for alginate, GelMA and GM/alg (n = 3, n represents number of hydrogel samples), related to Figure 7.

Figure S12. The scaffolds were retrieved from the surrounding tissue after 1-, 2-, 3-, and 4-weeks post implantation, related to Figure 7. A.) Process of multiscale composite scaffold implantation into the subcutaneous tissue of SD rats. B.) Scaffolds extracted along with the surrounding tissues after 1-, 2-, 3-, and 4-weeks following implantation.

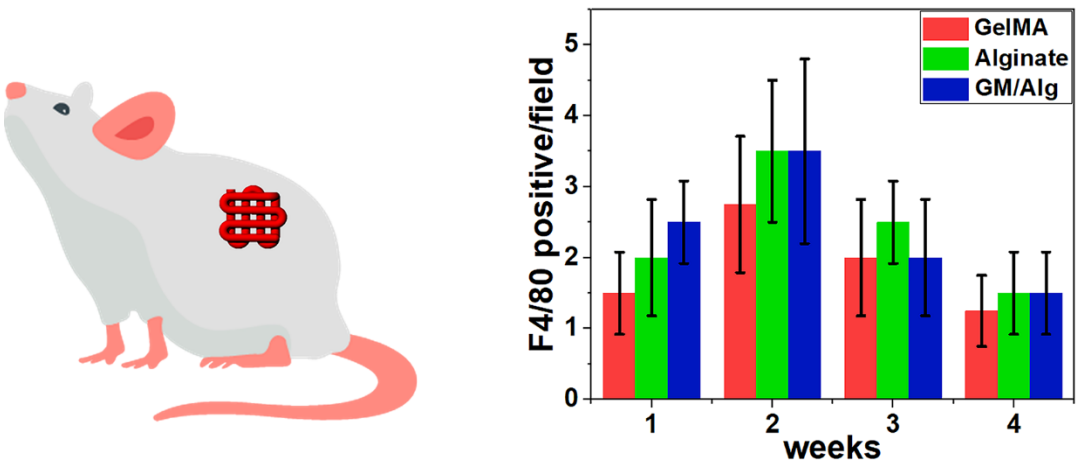

Figure S13. Schematic image of a rat with the implanted scaffold (left) and results obtained after different durations (right), related to Figure 7. Four different histological images were obtained from each section and used to analyze cell averages (n = 3, n represents number of cells).

Table S1. Properties of monodisperse GA microspheres with different diameters, related to Figure 3.

group	water phases (uL/min)	oil phases (uL/min)	flow rate ratio (I/O)	diameter (um)
I	10	300	1:30	330+19
II	10	600	1:60	214+12
III	10	900	1:90	160+6
IV	10	1200	1:120	128+4
V	10	1500	1:150	88+5
VI	5	900	1:180	130+4
VII	15	900	1:60	197+10